Accepted Manuscript

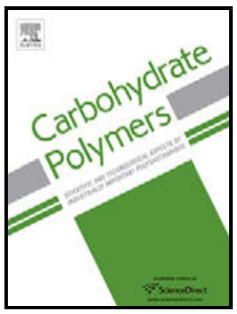

Title: Extrusion Induced Low-Order Starch Matrices: Enzymic Hydrolysis and Structure

Author: Bin Zhang Sushil Dhital Bernadine M. Flanagan Paul Luckman Peter J. Halley Michael J. Gidley

PII: S0144-8617(15)00733-X
DOI: http://dx.doi.org/doi:10.1016/j.carbpol.2015.07.095
Reference: CARP 10197

To appear in:

Received date: 25-5-2015
Revised date: 27-7-2015
Accepted date: 29-7-2015

Please cite this article as: Zhang, Bin., Dhital, Sushil., Flanagan, Bernadine M., Luckman, Paul., Halley, Peter J., & Gidley, Michael J., Extrusion Induced Low-Order Starch Matrices: Enzymic Hydrolysis and Structure.*Carbohydrate Polymers* http://dx.doi.org/10.1016/j.carbpol.2015.07.095

Extrusion Induced Low-Order Starch Matrices: EnzymicHydrolysis and Structure

Bin Zhang[a, †], *Sushil Dhital*[a], *Bernadine M. Flanagan*[a], *Paul Luckman*[b], *Peter J. Halley*[b], *Michael J. Gidley*[a, *]

[a]Australian Research Council Centre of Excellence in Plant Cell Walls, Centre for Nutrition and Food Sciences, Queensland Alliance for Agriculture and Food Innovation, The University of Queensland, St. Lucia, Brisbane, QLD 4072, Australia

[b]School of Chemical Engineering, and Australian Institute for Bioengineering and Nanotechnology, The University of Queensland, St. Lucia, Brisbane, QLD 4072, Australia

* Corresponding author. Phone: +61 7 3365 2145; Fax: +61 7 3365 1177. Email address:m.gidley@uq.edu.au(M. J. Gidley)

† Current address:Whistler Center for Carbohydrate Research and Department of Food Science, Purdue University, West Lafayette, Indiana 47907, USA (Email address: binzhang@purdue.edu)

E-mail addresses: binzhang@purdue.edu (B. Zhang); s.dhital@uq.edu.au (S. Dhital); b.flanagan@uq.edu.au (B. M. Flanagan); p.luckman@uq.edu.au (P. Luckman); p.halley@uq.edu.au (P. J. Halley); m.gidley@uq.edu.au (M. J. Gidley)

Abstract

Waxy, normal and high-amylose maize starches were extruded with water as sole plasticizer to achieve low-order starch matrices. Of the three starches, we found that only high-amylose extrudate showed lower digestion rate/extent than starches cooked in excess water. The ordered structure of high-amylose starches in cooked and extruded forms was similar, as judged by NMR, XRD and DSC techniques, but enzyme resistance was much greater for extruded forms. Size exclusion chromatography suggested that longer chains were involved in enzyme resistance.We propose that the local molecular density of packing of amylose chains can control the digestion kinetics rather than just crystallinity, with the principle being that density sufficient to either prevent/limit binding and/or slow down catalysis can be achieved by dense amorphous packing.

Keywords:high-amylose starch, extrusion, in vitro digestion, enzyme-resistant starch, local molecular density

Abbreviations

CP/MAS,cross-polarized magic angle spinning;DSC, differential scanning calorimetry/calorimeter; G50, Gelose 50; NMR, nuclear magnetic resonance; LOS, log of slope; NMS, normal maize starch;SEC, size exclusion chromatography; SEM, scanning electron microscope;WMS, waxy maize starch; XRD, X-ray diffractometry/diffractometer.

1. Introduction

As a majormacronutrient in human diets, starch is converted to glucose bythe mammalianenzyme system(i.e., α-amylases and mucosal α-glucosidases)and absorbed in the small intestine, and often provides more than 50% of total caloric intake (Nishida, Uauy, Kumanyika, & Shetty, 2004).Fast digestion of starch-containing foodsmay contribute to general chronic diseases in people such as type II diabetes, obesity, and cardiovascular disease. In contrast, starchwith slow digestion rate has been proposed to control glycemic responseand insulin secretion, and (partially)passesto the large intestineas resistant starch where it functions as a carbon sourceto stimulate bacterial fermentation, producing metabolites such as short-chain fatty acids(Englyst & Cummings, 1985). In order to eliminatecomplex intrinsic host factors and individual diversity, resistant starch is most commonly measured by *in vitro* methods that simulate *in vivo* conditions of starch digestion and referred to as 'enzyme-resistant starch (ERS)'(to distinguish it from true RS which is defined as the amount of starch that escapes digestion in the small intestine and therefore passes to the large intestine)(Chanvrier, Uthayakumaran, Appelqvist, Gidley, Gilbert, & Lopez-Rubio, 2007),particularly to elucidate structure-digestibility relationshipsforstarch-containing food.

While rapidly, slowly digestibleand resistant starch fractions in the current classification suggested by Englyst and Cummings (1985) have been widely used,recent evidence suggests that ERS can be better expressed as a kinetic phenomenon rather than a thermodynamically defined entity (Butterworth, Warren, Grassby, Patel, & Ellis, 2012; Htoon, Shrestha, Flanagan, Lopez-Rubio, Bird, Gilbert, et al., 2009; Zhang, Dhital, & Gidley, 2013).For example, potato starch granules (a 'resistant' starch) are not completely resistant to hydrolysis when subjected to higher enzyme concentrations, although the digestion rate is slow(Warren, Zhang, Waltzer, Gidley, & Dhital, 2015).The presence of amorphous material in enzyme-resistant fractions also confirms that the resistance is not simply based on a specific crystalline structure that is completely undigested

(Lopez-Rubio, Flanagan, Shrestha, Gidley, & Gilbert, 2008).Kinetic analysis of digestion is a powerful tool to understand heterogeneous reactions between complex starch substrates and enzymes. There are two types of rate-limiting stepswhich can determineenzymic digestion kinetics: (i) enzyme access/binding limited by physical barriers (e.g., intact plant tissues, whole grains and complex food products); (ii) enzyme catalysislimited by starch structural features, such as chemically modified starch, and crystalline/ordered forms such as retrograded starch and starch-lipid complexes. The ERS classification based on mechanisms to achieve lower digestion rate/extent has been recently reviewed (Dhital, Warren, Butterworth, Ellis, & Gidley, 2015; Zhang, Dhital, & Gidley, 2015).Although it has been generally accepted that crystallinity playsa major role in determining ERS in the absence of non-starch physical barriers, recent evidence has shown that apparent crystallinity of native starches is not directly linked with the percentage of ERS obtained after extrusion(Chanvrier, Uthayakumaran, Appelqvist, Gidley, Gilbert, & Lopez-Rubio, 2007; Htoon, et al., 2009; Shrestha, Ng, Lopez-Rubio, Blazek, Gilbert, & Gidley, 2010).Htoon, et al. (2009)reported that highlyamorphous extruded high-amylose maize starches could deliver high ERS contents *in vitro*.Even for native starch granules, crystallinity alone cannot explain their relative resistance to digestion (Zhang, Ao, & Hamaker, 2006).Therefore, there should be additional mechanisms involved in the formation of enzyme-resistant fractions apart from crystallinity. We hypothesise that the local molecular density of starch chains, in both native and processed starches, can control the digestion rate and extent. Although crystallintyis one way to achieve local molecular density, it appears that non- or weakly- crystalline chains can also pack in an equally enzyme-resistant form, the details of which are currently poorly understood.

Extrusion is a commoncommercial processing technique forstarch-based foods such as pasta and breakfast cereals. The main advantages of extrusion processing include the ability to handle viscous polymers in the presence of plasticizer(normally waterin food use). Similarly, the combination of a

high temperature with a large amount of mechanical energy input during a short time period canbe used to promotestructural changesof starchsuch as gelatinization, melting, degradation and fragmentation (Lai & Kokini, 1991).Generally, molecular, supramolecular and granular structures are disrupted by thermal (barrel temperature), humidity (plasticizer content) and energy input(e.g., screw speed, feeding rate, die size and screw configuration) during extrusion cooking, each of which could be expected to increase the accessibility of degrading enzymes to starch polymersin extruded products.The intense shear regime within the extruder can cleave α-(1→4), α-(1→6)-bonds as well asstarchordered structures such as crystallites and double helices. Amylopectin (highly branched large molecule) is degraded to a larger extent than the essentially linear and lower molecular weightamylose, and the degradation of amylopectin mainly occursin the outer branch chains (Liu, Halley, & Gilbert, 2010).The larger molecules of amylopectin together with high branching density and short branch length are associated with higher susceptibility to shear degradation (Liu, Halley, & Gilbert, 2010). Fragmentation of starch during extrusion depends on the operating conditions of the extruder such as screw speed, temperature, and moisture content as well as the type of starch used.

In the current study, we aim to understand the structural origins of enzyme resistance, especially from (near) amorphous conformations using starch extrudates and cooked starchesas model systems. For this purpose, three maize starches with different amylose contents were extrudedwith water as a sole plasticizer, and *in vitro* digestion kinetic profiles of starch extrudateswere examined.On the basis of the molecular and microscopic structures of initial extrudates and digestion remnants, mechanisms of enzyme resistance from starch matrices with non- or low-order conformations are discussed.

2. Materials and Methods

2.1 Materials

Three commercial starches, i.e., waxy (WMS), normal (NMS), and high-amylose (Gelose 50, G50) maize starches, were used in this study. NMS was from New Zealand Starch Ltd., (Auckland, New Zealand), and the other two starches were purchased fromIngredion Pty. Ltd., (Lane Cove, NSW, Australia). The apparent amylose contents of WMS, NMS, and G50 were found to be 0.1%,27.5%, and 56.8%, respectively, using an iodine colorimetric method (Hoover & Ratnayake, 2001).Porcine pancreatic α-amylase (A3176, activity 23 units/mg) and other chemicals were obtained from Sigma-Aldrich (St. Louis, MO, USA).

2.2 Extrusion Processing

Theextrusion processing was performed on a HaakePolylab co-rotating twin-screw extruder (Thermo Fisher Scientific, Karlsruhe, Germany) equipped with a 3 mm diameter cylindrical dieat a constant feed rate of 0.4 kg/h. The screw diameterwas 16 mm, and thelength/ diameter ratio was 42:1. Theextruder configuration, temperature profile and interval assignment of the extruder barrel are shown in Figure 1. For WMS and NMS, the barrel temperatureprofile was set at 105, 115, 125, 130, 130, 130, 130, 125, 120 (last barrel), and 105 (die block)°C, and the screw speed was set at 60 rpm, and plasticizer (water) content was 35 wt%. In order to achieve gelatinizationfor the more thermally-stable G50 starch, higher temperature profiles (105, 120, 135, 150, 150, 150, 150, 135, 120, and 105 °C), water content and screw speedswere used (45 wt% and 80 rpm for batch 1; 50 wt% and 60 rpm for batch 2).Allprocess parameters were automatically recorded by HaakePolysoftsoftware (Thermo Fisher Scientific, Karlsruhe, Germany). Samples were collected when a steady motor torque was reached, then immediately frozen in a liquid nitrogen bath,freeze-dried toavoid any further retrogradation, and ground using a cryogenic mill (Freezer/Miller 6850, Metuchen, NJ, USA)for further digestion and structural analysis.In order to elucidate the particle size effect on digestion properties, the NMS and G50 extrudates were segregated by size using seven screen sieves (size: 20, 32, 53, 75, 90, 125 and 150 µm,Labtechnics, Kilkenny, Australia) under gravity with mechanical

agitation using a sieve shaker (Labtechnics, Kilkenny, Australia).

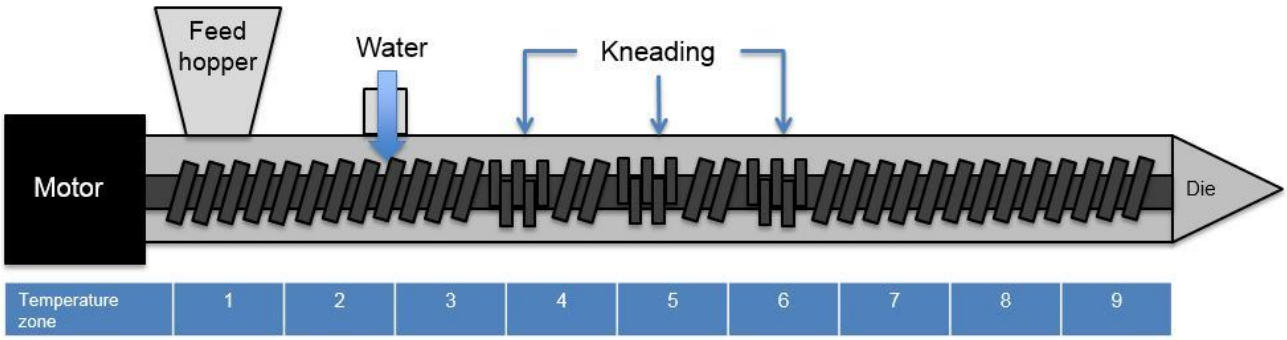

Figure 1.Scheme of the extrusion system used in this study. (The barrel temperatureprofile for WMS and NMS: 105, 115, 125, 130, 130, 130, 130, 125, 120 (last barrel), and 105 (die block) °C; the temperature profile for the G50 starch: 105, 120, 135, 150, 150, 150, 150, 135, 120, and 105 °C)

2.3 *In Vitro* Starch Digestion and First-OrderKinetics

The *in vitro* starch digestion procedurewas adapted from the method described byButterworth, Warren, Grassby, Patel, and Ellis (2012)with slight modifications. Starch extrudate(~50 mg, dry basis) wasincubated in 15 mL phosphate buffered saline (PBS)with 3.4 unitsα-amylase at 37°C with constant mixing. For the control groups, starches were cooked at 100°C for 30 min in 15 mL PBS buffer with constant mixing, and cooled down to 37 °C before adding the enzyme solution.At timed intervals up to 120 min, 300 µL of aliquot wasmixed with 300 µL of ice-cold sodium carbonate solution (0.5 M) to stop the reaction, and centrifuged at 16,000 g for 5 min to remove undigested starch. The concentration of maltose equivalent (reducing sugar)in the supernatant was determined bythe*para*-hydroxybenzoic acid hydrazide (PAHBAH) assay (H9882, Sigma)(Moretti & Thorson, 2008), and the maltose equivalent released (%)was calculated as follows.

$$\text{maltose equivalent released (\%)} = \frac{\text{total weight of equivalent maltose in supernatant}}{\text{dry weight of starch}} \times 100 \quad (1)$$

All digestion results were expressed as means of triplicate measurements. The undigested starch residues collected as precipitates after centrifugation were washed twice with de-ionized water, then

freeze-dried for further microscopic and structural analysis. The reducing sugar profile or digestogram was then fitted tofirst-order equation(using log of slope (LOS) plots) for the starch digestion kinetics as follows(Butterworth, Warren, Grassby, Patel, & Ellis, 2012):

$$\ln\left(\frac{dC}{dt}\right) = \ln(C_\infty k) - kt \quad (2)$$

where*t* is the digestion time (min), *C* is digested starch at incubation time *t*,C_∞ is digestion at infinite time, and *k* is rate constant (min^{-1}).Theplot of ln(d*C*/d*t*) against digestion time *t* is linear with a slope of –*k*, and the C_∞ can be calculated from the intercept of the equation and slope *k*. The rate constant is a function of the fixed amylase and starch concentrations used in the digestion, and is therefore pseudo-first order. The physical structure of starches also plays an important role in determining the rate constant of starch digestion(Zhang, Dhital, & Gidley, 2013).

2.4 Separation of Soluble and Insoluble Fractions

A starch sample (~50 mg, dry basis) was incubated in 15 mL water at 37 °C for 30 min with constant mixing. The suspension was then centrifuged at 4000 g for 10 min. The pellet (i.e., insoluble fraction) and the supernatant (i.e., soluble fraction) were frozen in a liquid nitrogen bath and dried using a freeze-dryer (VirTisBenchtop 4K, SP Industries, Inc., Warminster, PA),

2.5 Microscopy

Light microscopy was performed using an Olympus BX-61 light microscope (Tokyo, Japan) under bright or polarized field. The dried starch sample was suspended with glycerol and placedon the microscope slide before covering with a coverslip, and theimages were recorded at 200X magnification. For scanning electron microscopy (SEM), the starch sample wassprayed onto a circular metal stub covered with a double-sided adhesive carbon tape, then coated with platinum by a sputter coater (Eiko IB3, Mito, Japan) for 3 min at 15 mA. The images were acquired using a Philips XL30 scanning electron microscope (Philips, Eindhoven, the Netherlands) under an accelerating

voltage of 5 kV.

2.6 Differential Scanning Calorimetry

To characterize the extent of starch transformation after extrusion or digestion, extrudates/digesta were analyzed by differential scanning calorimetry (DSC, DSC 1, Mettler Toledo, Schwerzenbach, Switzerland) following the method ofB. Zhang, Huang, Luo, and Fu (2012). Starch samples (~5 mg) were mixed with de-ionized water to a moisture content of 70%, and hermetically sealed in a stainless steel pan. The scan was carried out from 20 to180°C at a heating rate of 10 °C/min. The enthalpy change (ΔH)as well as themelting (T_m) temperature wasdetermined from the thermograms by STARe software (Mettler Toledo, Schwerzenbach, Switzerland).

2.7 Wide Angle X-Ray Diffractometry

X-ray diffraction measurements were performed with an X'Pert Pro X-ray diffractometer(XRD) (PANalytical, Almelo, the Netherlands) operating at 40 kV and 40 mA with Cu Kα radiation (λ) at 0.15405 nm. The scanning region was set from 3 to 40° of the diffraction angle 2θwitha step interval of 0.02° and a scan rate of 0.5°/min. Thecrystallinepeak area and amorphous area were separated by PeakFit software (Version 4.12, Systat Software Inc., San Jose, CA, USA) following the method of Lopez-Rubio, Flanagan, Gilbert, and Gidley (2008). Relativecrystallinity was calculated as the ratio of the crystalline peak area to the total diffraction area.

2.8 ^{13}C CP/MAS Nuclear Magnetic Resonance Spectroscopy

Starch extrudates were analyzed by ^{13}C cross-polarized magic angle spinning (CP/MAS) nuclear magnetic resonance (NMR) spectroscopy before and aftersubsequent enzymic digestion, using a Bruker MSL-300 spectrometer (Bruker, Billerica, MA, USA) at a frequency of 75.46 MHz. Approximately 200 mg starch was packed in a 4-mm diameter, cylindrical, PSZ (partially stabilized

zirconium oxide) rotor with a Kel-F end cap. The rotor was spun at 5 kHz at the magic angle (54.7°). The 90° pulse width of 5 μs and a contact time of 1 ms were used for all starches with a recycle delay of 3 s. The spectral width was 38 kHz, acquisition time 50 ms, time domain points 2 k, transform size 4 k, and line broadening 20 Hz. At least 1000 scans were accumulated for each spectrum. Spectral acquisition and interpretation methodology as described by Tan, Flanagan, Halley, Whittaker, and Gidley (2007) were used to quantify the double helices, single helices, and amorphous conformational features.

2.9 Size Exclusion Chromatography

The whole (fully branched) and debranched size distribution of starch molecules were analyzed by a size exclusion chromatography (SEC) system (Agilent 1100, Agilent Technologies, Waldbronn, Germany) equipped with a refractive index detector (RID-10A, Shimadzu, Kyoto, Japan) following the method of Cave, Seabrook, Gidley, and Gilbert (2009) andB. Zhang, Dhital, Flanagan, and Gidley (2014) with minor modification.For fully branched size distribution, starch (2 mg) was dissolved in 1 mL DMSO solution containing 0.5% (w/w) LiBr (DMSO/LiBr) at 80 °C in a thermomixer (Eppendorf, Hamburg, Germany) for 24 h. Samples were mixed well and centrifuged at 4000g for 10 min. Supernatant was transferred into a SEC vial then injected into the following series of columns: precolumn, Gram30, and Gram3000 (PSS, Mainz, Germany). The injection volume was 100 μL, the flow rate was 0.3 mL/min, and the temperature was 80 °C. For debranched size distribution, starch (~ 4 mg) was dissolved in 1.5 mL DMSO/LiBr in the same way as that of the fully branched samples. The dissolved starch was then precipitated using 6 mL absolute ethanol. The recovered starch pellet was dissolved in 0.9 mL of warm deionized water in a boiling water bath for 15 min. After being cooled to room temperature, the starch dispersion was mixed with 5 μL sodium azide solution (40 mg/mL), 0.1 mL acetate buffer (0.1M, pH 3.5), and 2.5 μLisoamylase (1000U/mL, Megazyme, Co. Wicklow,Ireland), in sequence, and the debranching reaction was carried out at 37

°C for 3 h. The debranched starch dispersion was neutralized to pH ~7 dropwise with 0.1 M NaOH solution, then heated in 80 °C water bath for 2 h to inactivate enzyme. Debranched samples were freeze-dried and comprised ~6 mg/mL starch in DMSO/LiBr, and were injected into PSS Gram100 and 1000 columns following a pre-column. The injection volume was 100 μL, the flow rate was 0.6 mL/min, and the temperature was 80 °C.

The molecular size distribution data were plotted as SEC weight distribution, $w(\log V_h)$ as a function of the hydrodynamic radius (R_h/nm).For branched starch molecules, there is no unique correspondence between size and molecule weight (Gilbert, Gidley, Hill, Kilz, Rolland-Sabate, Stevenson, et al., 2010).For linear polymers of uniform geometry, the size and molecular weight (or equivalently the degree of polymerization, DP) are uniquely related, and hence the size distribution can be converted to a molecular weight distribution using the Mark-Houwink equation(Cave, Seabrook, Gidley, & Gilbert, 2009; Clay & Gilbert, 1995).The Mark-Houwink parameters K and $\alpha$for linear starch polymers in DMSO/LiBr at 80 °C are 0.0150 mL/gand 0.743, respectively(Liu, Halley, & Gilbert, 2010).

2.10 Statistical Analysis

Results were expressed as means of duplicate measurements unless otherwise specified. Analysis of variance (ANOVA) was used to determine significance at $p< 0.05$ using Minitab 16 (Minitab Inc., State College, PA, USA),and correlation coefficients were determined using Microsoft Office Excel 2013.

3. Results

3.1 *In Vitro*Starch Digestion

In vitro digestion kinetic profiles of control (i.e., cooked starches) and experimental (i.e., starch extrudates) groups were monitored by reducing sugar assay with a fixed α-amylase activity;results areshown in Figure 2A. The digestion rate and extent ofstarch or starch-containing food are very dependent on the enzyme type(s) and the concentration conditions used (Warren, Zhang, Waltzer, Gidley, & Dhital, 2015). For example, α-amylase and amyloglucosidaseact synergistically in the production of glucose from granular starch digestion, whereas there is an antagonistic effect for cooked starches (Zhang, Dhital, & Gidley, 2013). Therefore, this kinetic study usedα-amylase alone to investigate digestion rate/extent of starches in cooked orextrudate forms. In order to obtain a logarithmic digestion curve andfit first-order kinetics, a selectedα-amylase activitycondition (3.4 unit per 50 mg starch) was used to convert sufficient starch substrate to oligosaccharide products over the time course, showing logarithmic curves for all starch samples(Butterworth, Warren, Grassby, Patel, & Ellis, 2012; Warren, Zhang, Waltzer, Gidley, & Dhital, 2015).It should be noted that the selectedamylase activity is dependent on the physical nature of a starch substrate; for example, a relatively higher amylase concentration is needed for native starches compared to cooked forms, and also depends on the botanic origins(Butterworth, Warren, Grassby, Patel, & Ellis, 2012; Zhang, Dhital, & Gidley, 2013).

LOS fitting analysis (shown inSupplementary Data Figure S1) was applied to the starch digestion kinetic profiles to obtain first-order coefficients (*k*), showing thatall digestion profiles can be describedbya single-phase pseudo-first order process (R^2> 0.90). Singlerate coefficients of starchesin cooked and extrudate forms and digestion extents after 2 h of digestion are summarized in Table 1. Comparison of the digestion rate and extent of WMS and NMS in cooked and extrudateformsindicated that the digestion processes (digestogram and *k* values, Figure 2A and Table 1) are similar, although NMS extrudate has a slightly lower reducing sugar value after 2 h of digestion (64.1%cf 69.1 - 72.2%),suggesting a role for amylose in reducing hydrolysis rates in

essentially non-ordered (Table 2) extrudatesamples..Compared to other cooked starches, cooked G50 starch shows slightly lower digestion rate and extent (0.0400 min^{-1}, 56.5%, respectively). However, it was found thatthe digestion rate coefficient for two G50extrudatebatches (batch one, 0.0238 min^{-1};batch two, 0.0244 min^{-1}) was ca. 2 times lower than that of WMS and NMS extrudates. In addition, among extrudates from different initial amylose contents, high-amylose starch shows relatively higher enzyme resistance towards amylase (yield of ERS at 2 h of digestion>40%), consistent with previous reports (Chanvrier, Uthayakumaran, Appelqvist, Gidley, Gilbert, & Lopez-Rubio, 2007; Htoon, et al., 2009).

In order to elucidate the effect of particle size on enzymic susceptibility, NMS and G50 extrudates were fractionated into various sizes by sieving,and analyzed for amylase digestion kinetics with results presentedin panelsB and C of Figure 2.Small and medium size fractions (32 – 125 μm) didnot affect the digestion kinetic profiles much (digestogram and *k* values). As shown in Supplementary Data Table S1, the majority (relative yields > ca. 85%) of extrudateswere in the small and medium size fractions, in agreement with their overall digestion kinetics. As the particle size increased, a marked reduction in starch digestibility for the larger size particles (>125 μm) of both NMS and G50 extrudates was observed.

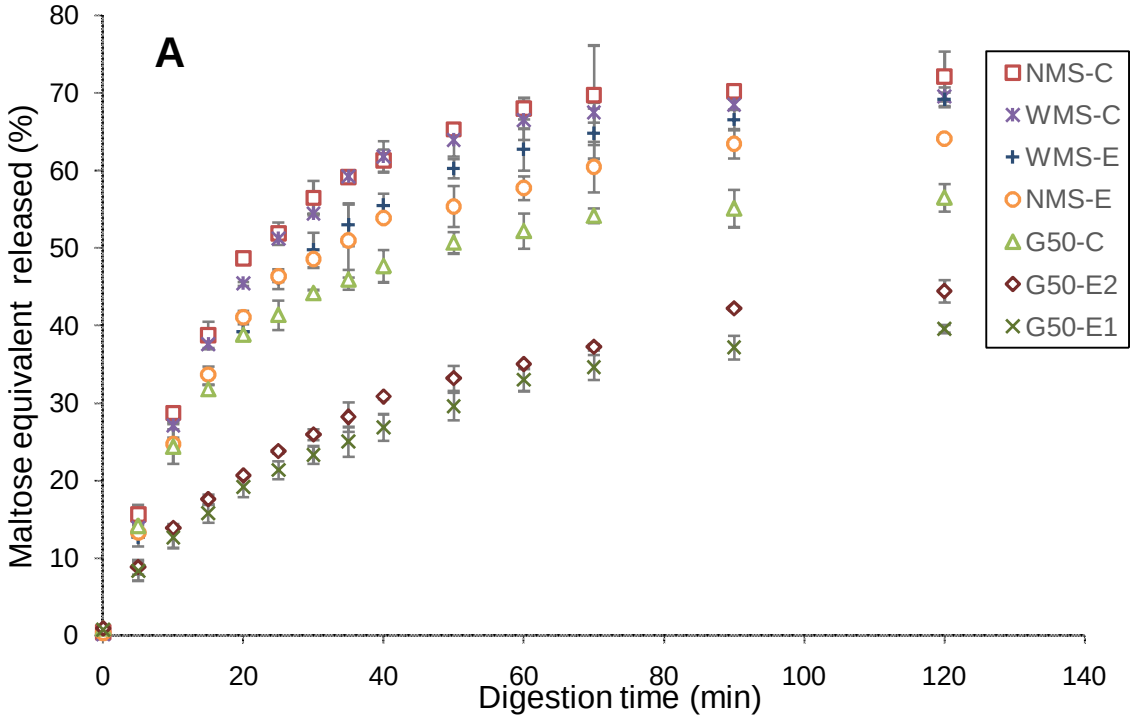

300

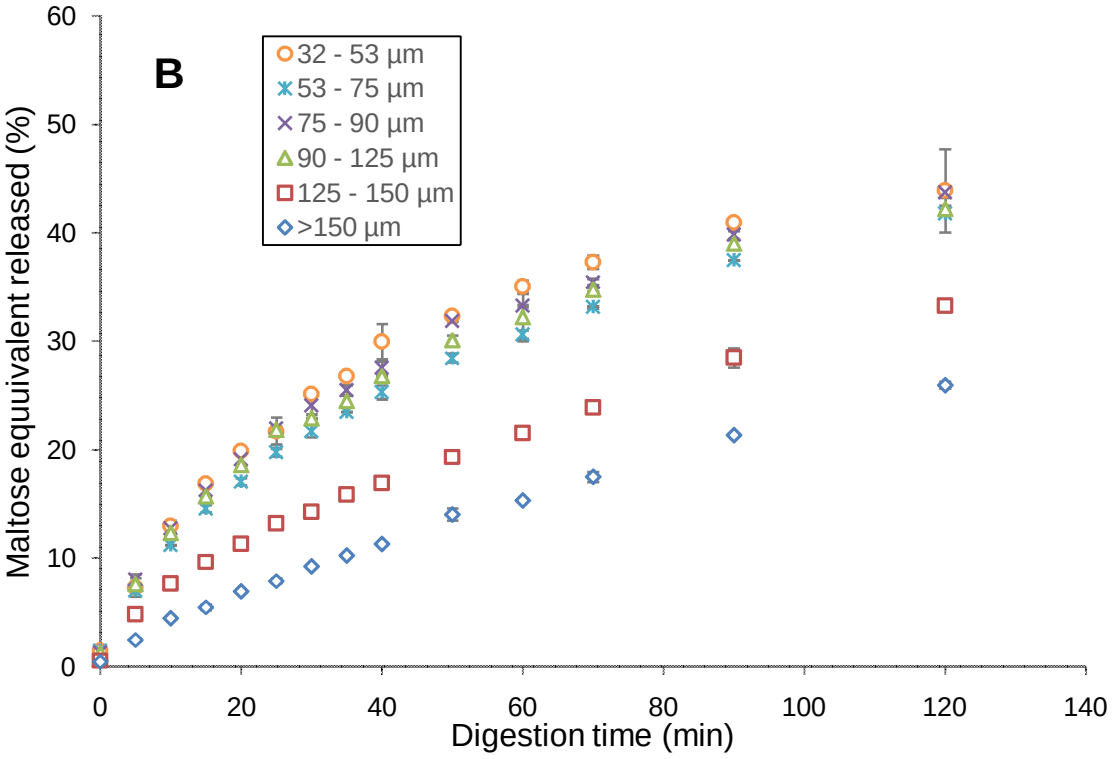

301

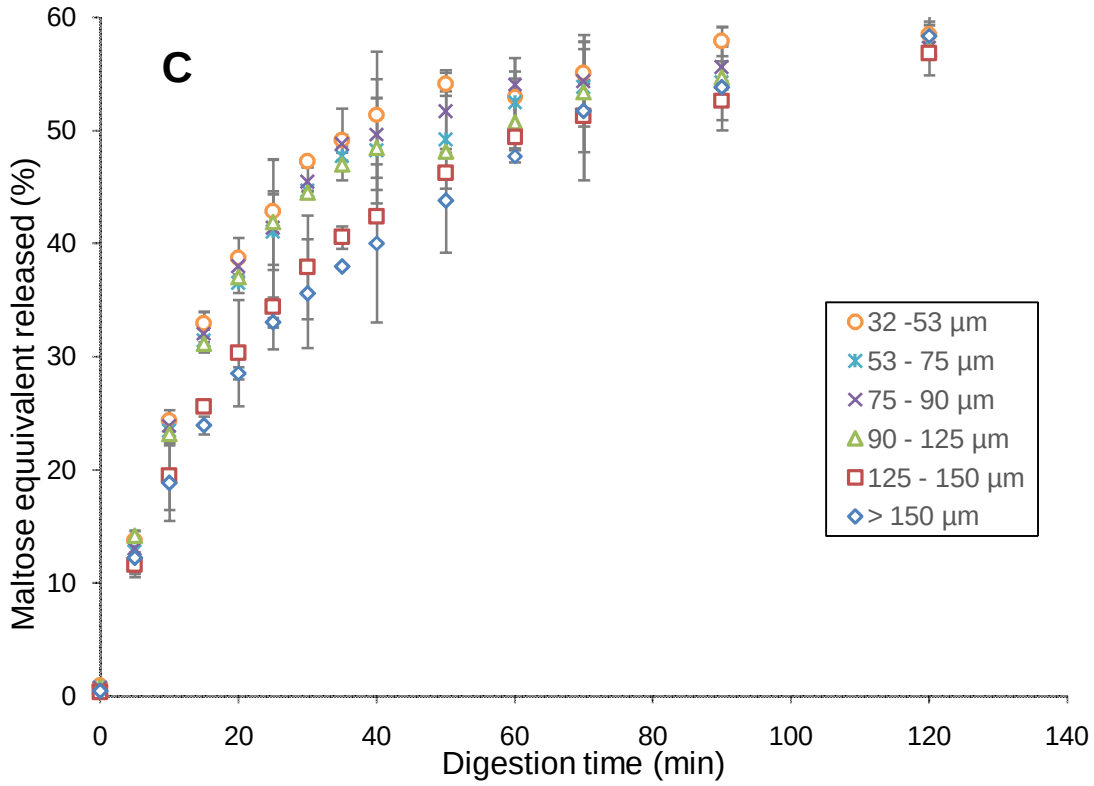

Figure 2. (A) Digestion kinetic profiles of waxy, normal and high-amylose maize starches subjected to cooking or extrusion processing. Digestion kinetic profiles of size fractionated extruded high-amylose (B) and normal (C) maize starches. (WMS, waxy maize starch; NMS, normal maize starch; G50, high-amylose maize starch; E, extrudate; C, cooked).

Table 1. Digestion rate coefficient (k, min^{-1}) and reducing sugar released extent after 2 h digestion of starchesin cooked and extrudateforms.[A] (WMS, waxy maize starch; NMS, normal maize starch; G50, high-amylose maize starch; E, extrudate; C, cooked)

sample	k(min^{-1})	Reducing sugar released (%)
WMS-C	0.0481	72.2(3.2) a
NMS-C	0.0447	69.6(1.2) a
G50-C	0.0400	56.5(1.8) c
WMS-E	0.0403	69.1(1.0) a
NMS-E	0.0408	64.1(0.3) b
G50-E1	0.0238	42.7(0.5) d
G50-E2	0.0244	44.5(1.4) d

[A]Means (standard deviations) from three measurements.Values in the column with different letters are significantly different at $p< 0.05$.

3.2 Microscopic Structure of Extruded Starches and Their Digestion Residues

Electron and light micrographs of extruded starches and residues/fragments after 2 h of digestion are shown in Figure 3. The G50 starch granules before extrusion (Figure 3 A1and B1) show spherical or occasional elongated rod (arrow in Figure 3 A1) shapes with apparently unimodalparticle size distribution ranging from 5 to 20 µm as reported previouslyfor maize starch granules of similar amylose content(Jiang, Horner, Pepper, Blanco, Campbell, & Jane, 2010).Under polarized light, native G50 starch granules show characteristic birefringence with clear Maltese crossescentered at the hilum (Figure 3 C1).From SEM and light microscopy (Figure 3 A2 – A4, B2 – B4), extrusion and cryo-milling resulted in both fragmentation and aggregation with a wide size distribution ranging from 10 to 200 µm. Although the WMS and NMSextrudates show condensed and irregularly-shaped surface structures under SEM, they could be partly dissolved in water or PBS buffer quickly (from experimental observations). No birefringence can be detectedfrom WMS and NMSextrudates(Figure

3 C2 – C3), suggesting that complete gelatinization is induced by extrusion.In contrast, extruded G50 starchesshow a low level of birefringence and distorted Maltese crosses (Figure 3 C4),indicating that the current extrusion conditions did not completely disrupt the ordered structure. A number of different extrusion conditions (e.g. maximum temperatures from 130°C to 150°C) and water contents (from 35 % to 50 %) were evaluated, but none were able to produce G50 extrudates lacking any birefringence. Complete melting of high-amylose starches by extrusion in the presence of non-aqueous plasticizers or solvents is possible(Xie, Flanagan, Li, Sangwan, Truss, Halley, et al., 2014), but for this study we limited ourselves to water as the only plasticiserof relevance to food processing. The observedstructure of G50 extrudates (Figure 3 A4)is similar to WMS and NMS extrudates (Figure 3 A2-3), but was constrained from swelling extensively in water or buffereven after enzyme treatment(Figure 3 B6) unlike WMS or NMS extrudates. By the end of the 2h digestion process, a marked reduction in particle size was observed compared to the initialG50 starches in cooked or extrudate form, as shown in panels A5 – A6 and B5 – B6 of Figure 3. Most digestion residues were present as smaller particles with a similar size of around 10 µm, along with a few large aggregates. Under polarized light, relatively lower levels of birefringence and some clear Maltese crosses can be identified from digesta of cooked or extrudedG50 starches(Figure 3 C5 – C6), indicating that the digestion remnants were composed of G50 granules tightly embedded in a starch matrix (extrudate) or residual granules with incomplete disruption of internal organization during extrusion or cooking.

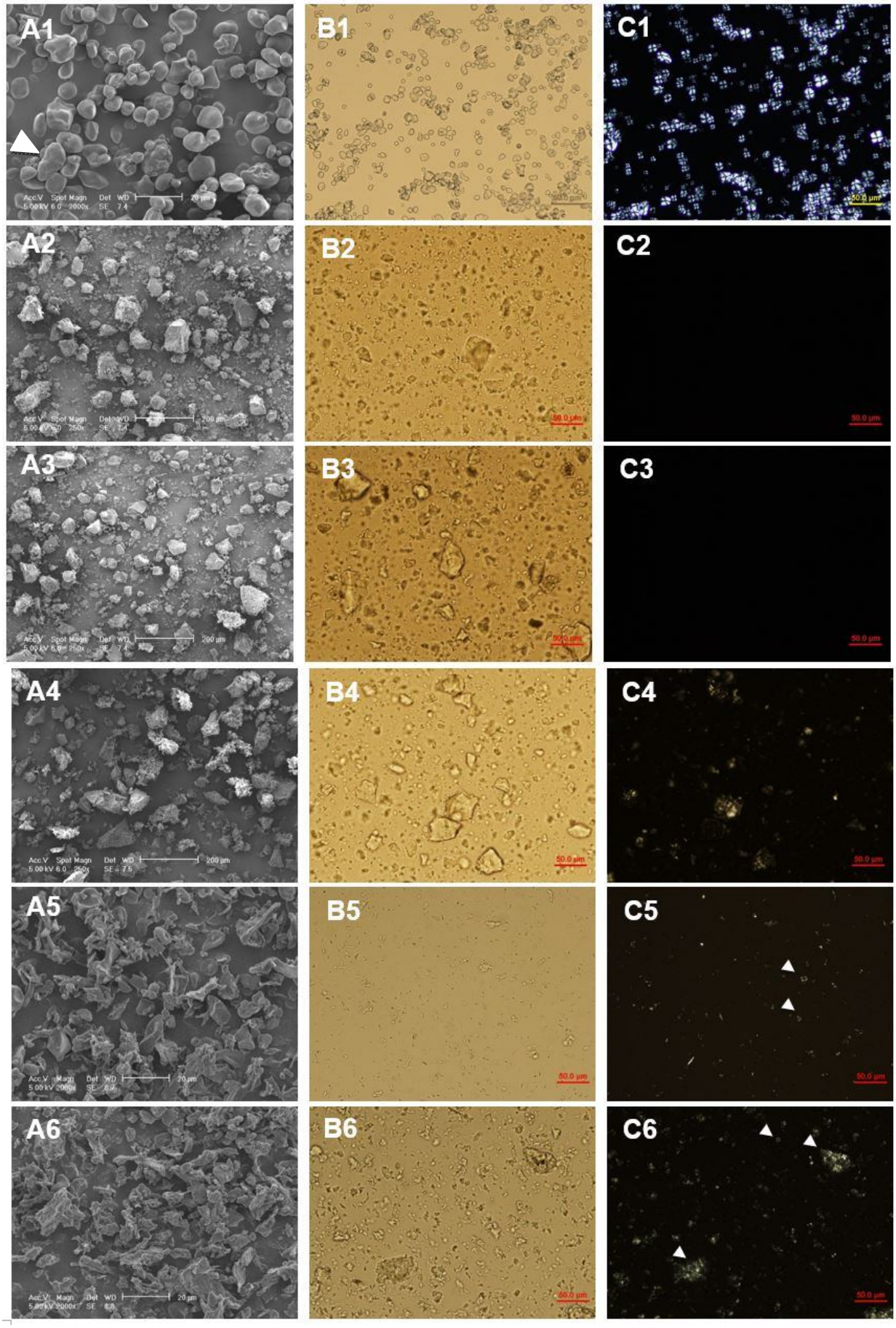

Figure 3. Micrographs (A, scanning electron micrographs; B and C, light micrographs under bright field and polarized light respectively) of extruded starches (1: native G50 starch; 2, 3, 4: extruded waxy, normal, and high-amylose maize starches respectively) and their 2 h digestion residues from cooked G50 (5) and extruded G50 (6) starches. Arrows show an elongated granule (A1) andrepresentative Maltese crosses of starch granules(C5, C6).

3.3 Molecular Order and Crystallinity Before and After Digestion

The molecular order (i.e., helical content) and crystallinity level of starch extrudates before and after enzymic hydrolysiswere quantified by solid-state NMRspectroscopy and XRD respectively, as shown in Figure 4 and Table 2.The melting (peak) temperature and enthalpy determined by DSC for different starch samples after extrusion and after 2 h of digestion,are summarized in Table 2. Extrusion processing under the selected condition leads to the almost completegelatinization of waxy and normal maize starches, as shown by<5% A-type double helices and <1% crystallinity (Table 2) as well as DSCthermogramswithout any endothermic peak up to 180^{o}C(data not shown)consistentwith the absence of birefringence in Figure 3 C2-3.As observed in Figure 4A, native high-amylose G50 starch displays a typical B-type diffraction pattern with major peaks at ~5, 14, 17, 22 and 24$^{o}2\theta$, and a clear peak at ~20$^{o}2\theta$ is ascribed to V-type single helices (Cheetham & Tao, 1998).However, V-type polymorph does not always imply a fatty acid complexed with amylose molecules(Godet, Buleon, Tran, & Colonna, 1993), and this formation is favored under high-shear extrusion conditions as reported elsewhere (Lopez-Rubio, Htoon, & Gilbert, 2007).After processing, the G50 extrudatesshowsmostly B-type polymorph with some clear evidencefor V-type peaks (e.g., at ~8, 13, 20$^{o}2\theta$, see Figure 4A)andabout 50% reduction of B-type double helix and crystallinity levels (Table 2), compared to the original native form.The DSCthermograms for extruded G50 starches had a board endothermic peak ranging from 113 to 130^{o}C and peaking at around 120^{o}C. In addition, the enthalpy of this peakwas very low and not significantly different from batch one to

384 batch two (between 1.5 and 1.9 J/g), which could be attributed to the melting of retrograded amylose
385 formed during extrusion.
386
387 The digestion residues of G50 starches in cooked and extrudate forms also show a mixture of B- and
388 V- type polymorphs from X-ray diffractograms (Figure 4A). Similar to the corresponding extrudate
389 samples, only B-type double helices were detected from NMRspectroscopy(Figure 4B),presumably
390 because of some randon coil-like amylose molecules without any inclusion formed during extrusion
391 as described previously(Godet, Buleon, Tran, & Colonna, 1993).The levels of molecular and
392 crystalline order were slightly higher for the ERS residues (~17% double helix and ~17%
393 crystallinity) than for the starting extruded G50 starches (9-12% double helix and 11-14%
394 crystallinity).The enzyme resistant B-type ordered helical structure could be from either accumulated
395 or newly formed double helices during the time course of digestion(Cairns, Sun, Morris, & Ring,
396 1995).Lopez-Rubio, Flanagan, Shrestha, Gidley, and Gilbert (2008)suggested that partly degraded
397 shorter amylose chains show high mobility, and can self-assemble into more enzyme resistant double
398 helices during digestion. However, it is noteworthy that the molecular order and crystallinity levels
399 of the digesta were close to the corresponding native G50 starch as shown in Table 2, showing that
400 still more than 80% of the 2h digestion residue fraction is amorphous.The melting temperature and
401 enthalpy of the digestion residues were slightly lower compared to starting G50 extrudates, probably
402 due to partial degradation of double helices by α-amylase.
403

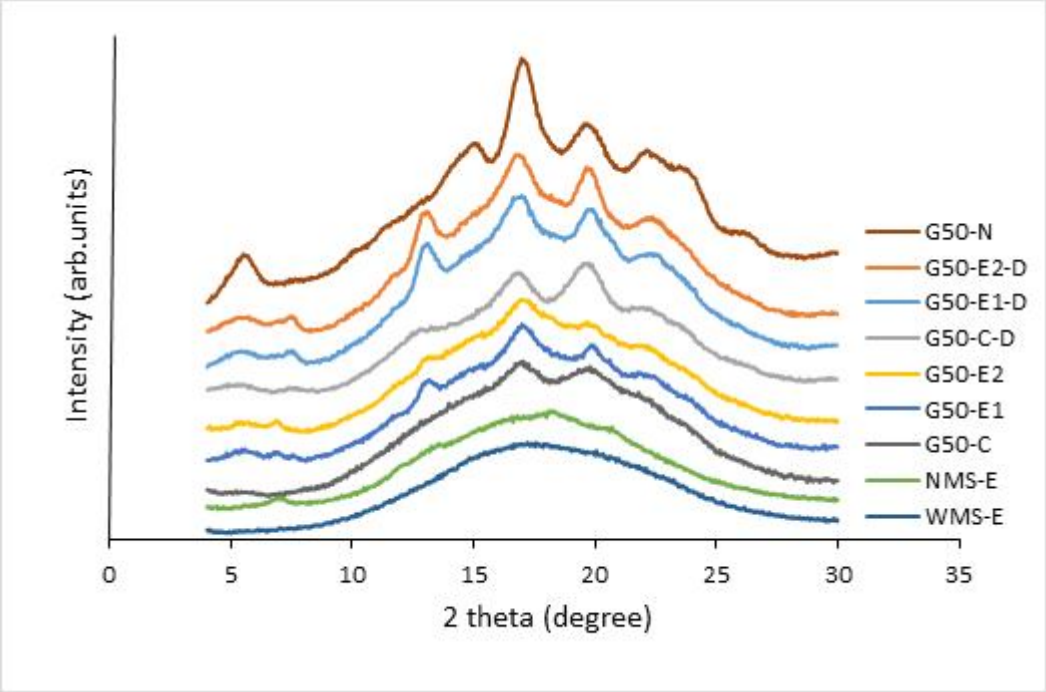

Figure 4A. X-ray diffractograms of extruded starches and their 2 h digestion residues (WMS, waxy maize starch; NMS, normal maize starch; G50, high-amylose maize starch; E, extrudate; N, native; C, cooked; D, 2 h digestion residue).

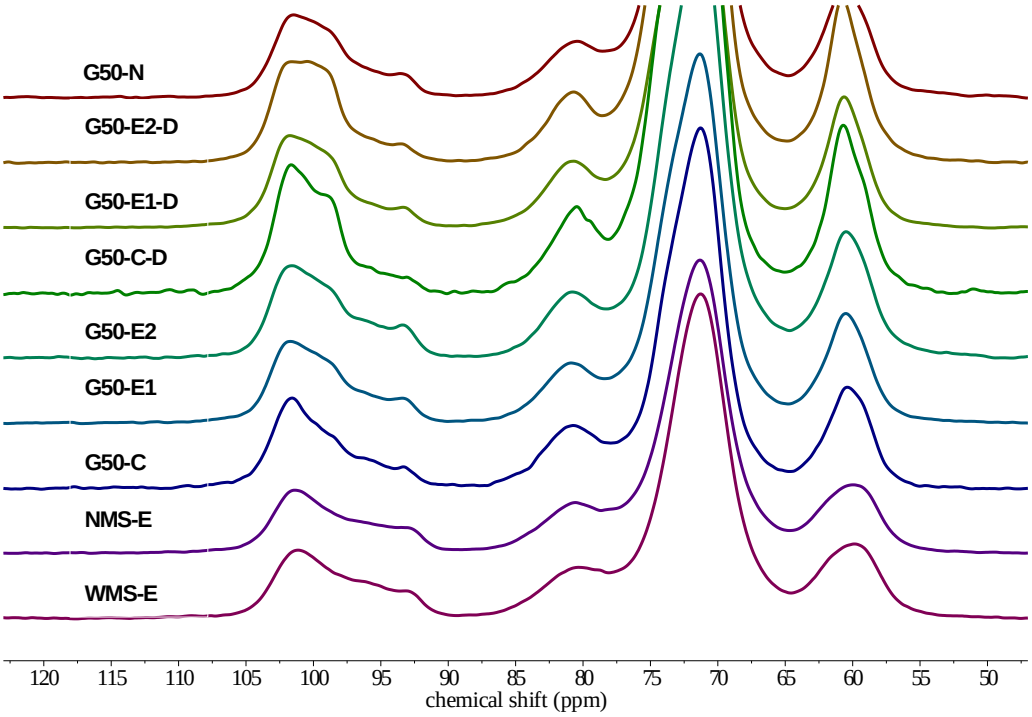

Figure 4B. Stacked plot of ^{13}C CP/MAS NMR spectra of starches, normalized at 84ppm. The C-1 peak at 93-107 ppm is particularly sensitive to molecular order.

Table 2. Molecular order, crystallinity and thermal properties of extruded starches and 2 h digestion residues.[A] (WMS, waxy maize starch; NMS, normal maize starch; G50, high-amylose maize starch; E, extrudate; N, native; C, cooked; D, 2 h digestion residue)

sample	^{13}C NMR		XRD		DSC	
	double helix (%)	single helix (%)	A-or B-type	V-type	T_m (°C)	ΔH (J/g)
WMS-E	4	0	<1	0	-	-
NMS-E	5	1	<1	3	-	-
G50-E1	12	0	14	3	118.8(0.7) b	1.9(0.1)bc
G50-E2	9	0	11	4	122.3(0.9) a	1.5(0.2) c
G50-N	22	5	26	3	79.8(0.3) e	9.8(0.4) a
G50-C	5	2	9	3	ND [B]	ND [B]
G50-C-D	21	0	14	8	102.5(0.3) d	2.7(0.2) b
G50-E1-D	17	0	17	8	115.1(0.7) c	1.3(0.1) c
G50-E2-D	16	0	17	6	115.6(0.6) c	1.2(0.1) c

[A] XRD and NMR calculations are within SD of 2%.Means ± standard deviations fromat least two measurements.Values in the same column with different letters are significantly different at $p<0.05$.$T_m$andΔH are melting temperatureand enthalpy change, respectively.

[B] Not determined.

3.4 Molecular Size Distributions

The molecular size distributions of enzymatically debranched and fully branched starch polymers were characterized using SEC. All SEC weight distributions were normalized to yield the same height of the highest peak to bring out detailed features and to facilitate qualitative comparison and interpretation, and are presented in Figures 5 and 6. Typical chain length distributions ofdebranchedstarch molecules (e.g., native G50 starch, Figure 5 A) showsbimodal peaks representing amylopectin branches (single-lamella, peak R_h ~1.5 nm or DP ~ 16; trans-lamella, R_h peak ~2.5 nm, DP ~50) and amylose branches (R_h ~5 – 80 nm, DP ~100 – 10000) (Wang, Hasjim, Wu, Henry, & Gilbert, 2014; Zhang, Dhital, Flanagan, & Gidley, 2014).The branched SEC weight distribution of native G50 starch (see Figure 5 E) exhibits two distinct peaks for amylose and amylopectin molecules separated at R_h ~200 nm.It is noteworthy that shear degradation of dissolved starch molecules in DMSO/LiBr happens during SEC separation, especially for amylopectin which is

sufficiently degraded to a smaller sizeto resultin overestimation of the amylose peak(Gidley, Hanashiro, Hani, Hill, Huber, Jane, et al., 2010).The fully branched SEC distribution of extruded G50 starch (Figure 5 F) shows aunimodal peak witha large reduction in amylopectin size. Degradation during extrusion preferentially operates on the large molecular size and highly branched primary structure of amylopectin, whereas whole amylose molecules could be largely retained(Liu, Halley, & Gilbert, 2010).The mechanical/shear force induced by extrusion processing is believed to randomly cleave glycosidic bonds in branches of amylopectin, but with more pronounced action adjacent to rigid crystallites in granular starches (Li, Hasjim, Xie, Halley, & Gilbert, 2014).This is consistent with the lack of qualitative difference in the debranched chain length distributions between native and extruded G50 starches, as shown in panels A and B of Figure 5.

The branched SEC weight distributions forsoluble starch fractionsshow a single peak with a smaller molecular size ($R_h$peak ~10 nm,Figure 6 E, G) compared to thebimodal peaksfor theinsoluble fractions of cooked and extruded G50 starches(Figure 6 E-H), indicating that these lower size molecules could bedissolved in water or PBS buffer before enzyme reaction happened. The branched SEC data of all extruded G50 samples in either soluble or insoluble form show slightly lower $R_h$peaks than corresponding cooked starches (Figure 6 E, G cf. F, H), consistent with the shear degradation mechanism discussed above. In addition, comparison of the debranched SEC data(Figure 6A - D) alsoshowsthat incubation of both cooked and extruded starches in the PBS buffer at 37^{o}C is accompanied by the partialdissolution of both amylose and amylopectin with low molecular size: less release of degraded polymers for the extrudate form and more for cooked G50 starch. Starch samples after 2h of amylase digestionwere greatly degraded in wholemolecular size (Figure5 G,H), and contained a mixture of amylopectin (R_h peak ~2 nm, DP ~25) and long chain polymers (R_h>~5 nm, DP >~100) interpreted from Figure 5C, D.There were more long chain polymers with R_h ~ 10 nm in the digestion residues from G50 extrudates (Figure 5 C cf. D) as well

as larger polymers (R_h> 10 nm; Figure 5 G cf. H), which might play important roles in restricting enzyme action.

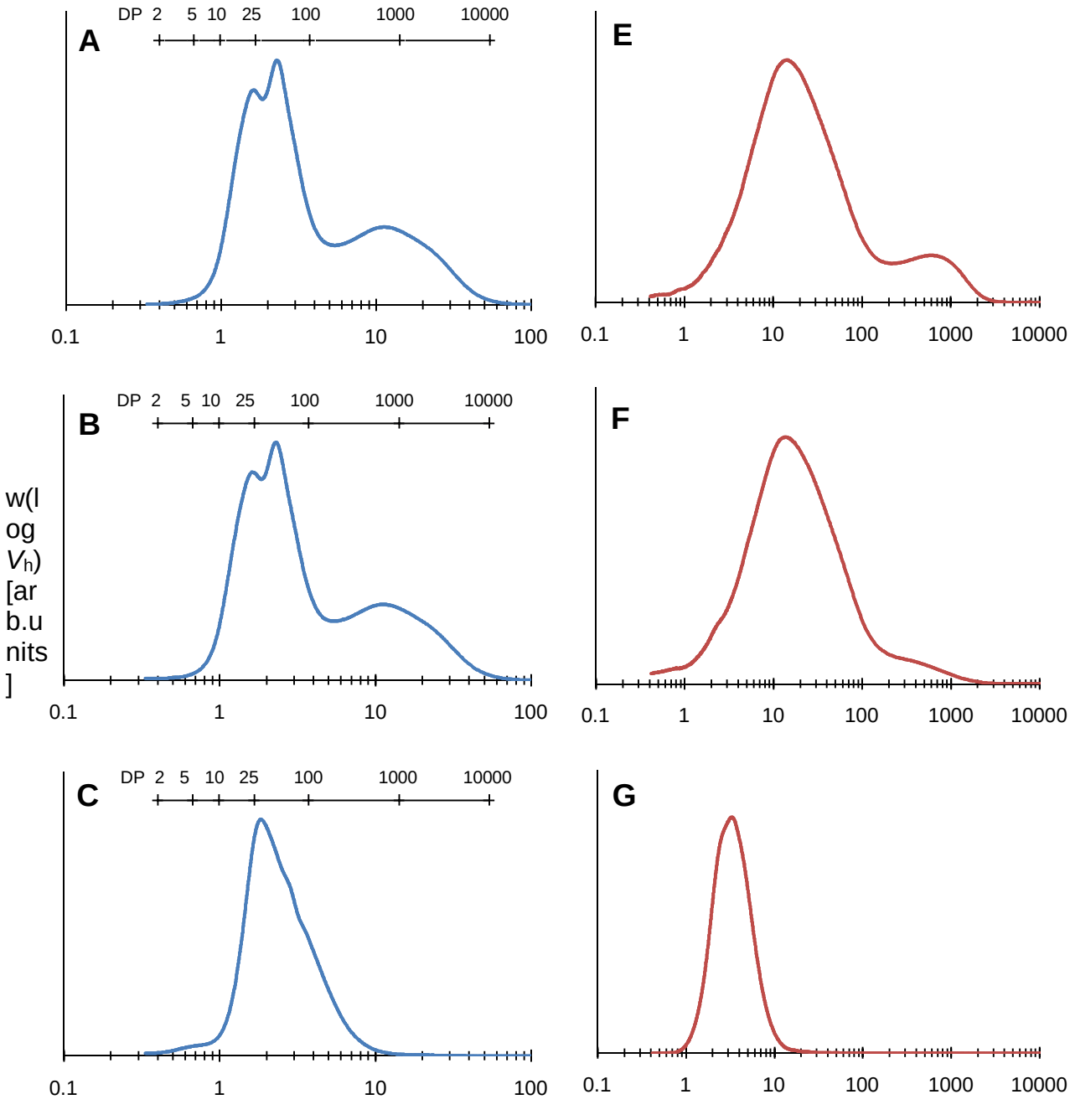

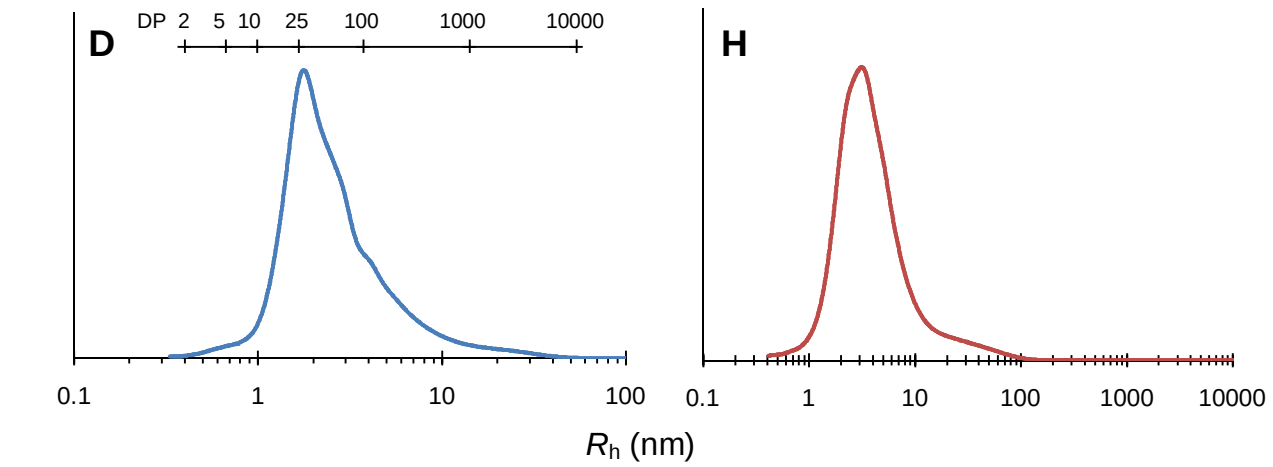

Figure5. Size distributions of debranched (A - D) and whole (E - H) molecules from native (A, E) and extruded (B, F) G50 starches and 2 h digestion residues of cooked (C, G) and extruded (D, H) G50 starches.

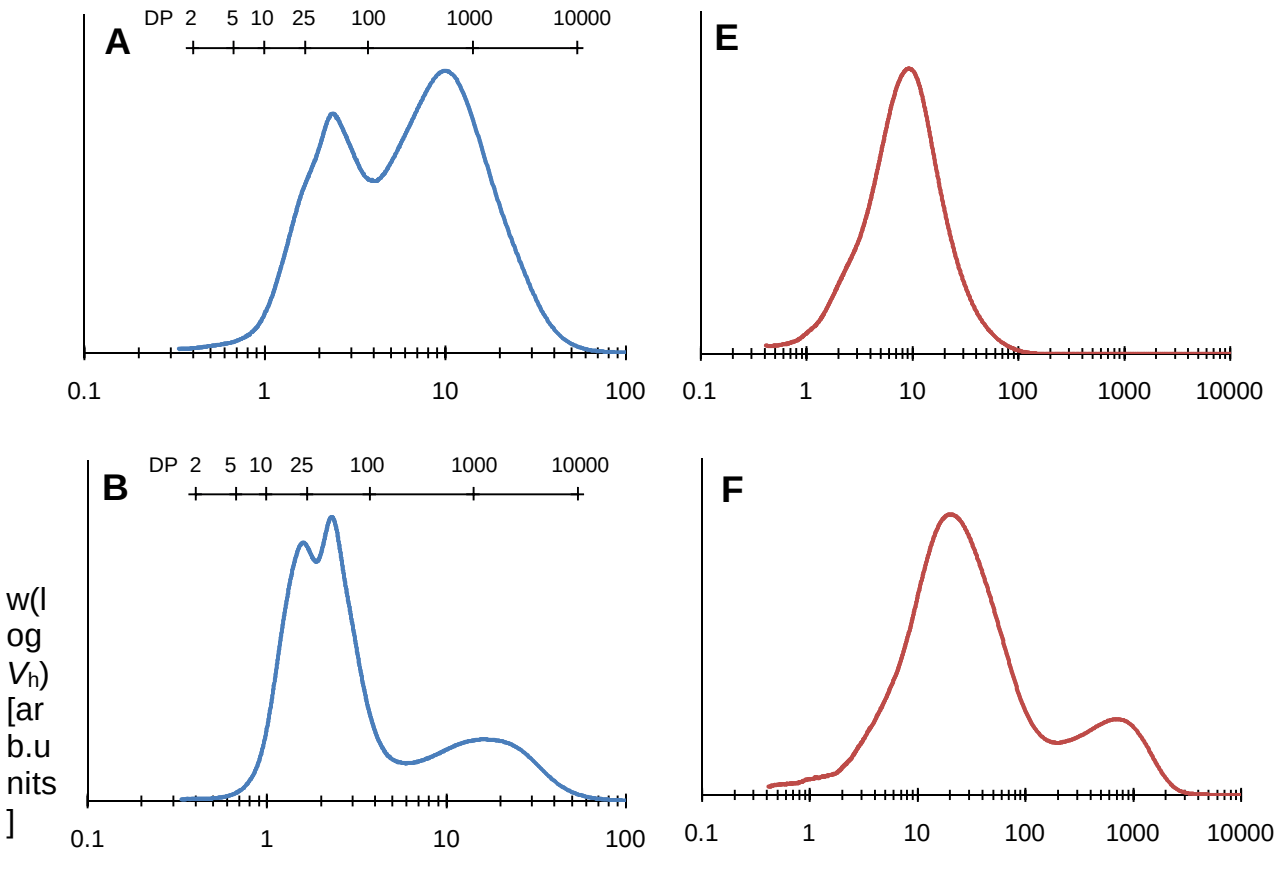

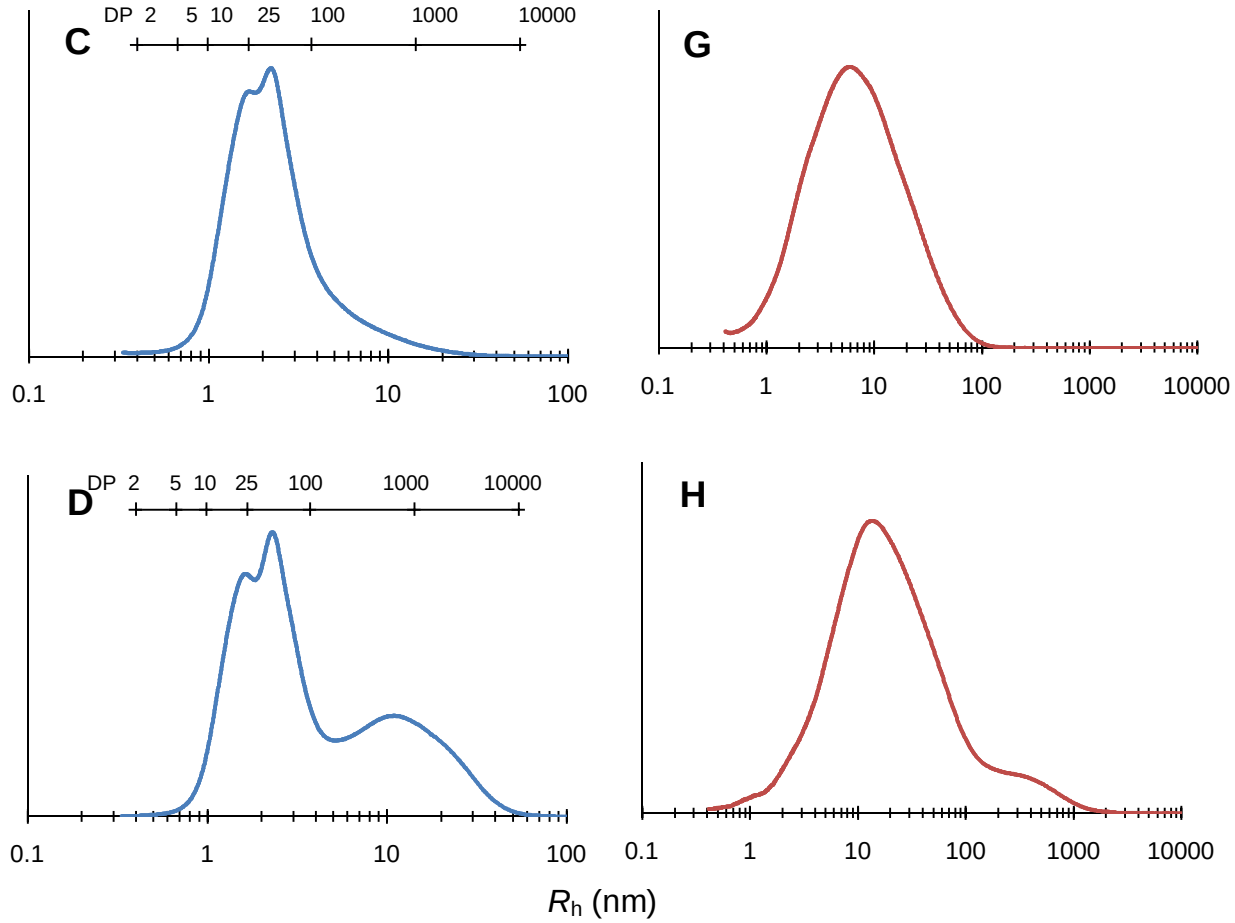

Figure6. Size distributions of debranched (A - D) and whole (E - H) molecules from the soluble fraction of cooked (A, E) and extruded (C, G) G50 starches, and the insoluble fraction of cooked (B, F) and extruded (D, H) G50 starches.

4. Discussion

Generally, molecular, crystalline, and granular structure of starchesfrom nanometer to micrometer length scales are disrupted by the intense thermo-mechanical energy inputof an extruder, which wouldbe expected to generate an amorphous structure and increase the accessibility of starch molecules for enzymic hydrolysis(Bird, Lopez-Rubio, Shrestha, & Gidley, 2009; Faraj, Vasanthan, & Hoover, 2004).Although the WMS and NMS extrudates have a densely-packed surface structure in the dried state (Figure 3 A2 - 3), the local molecular density of starch matrices is temporary and is lost when subject to hydration, leading to higher digestion rate and extent compared to

G50extrudate.Therefore, there was no difference in digestion rate coefficients between WMS incooked and extrudate formsand only a small (but significant) difference for NMS, as shown in Table 1.Incompletegelatinizationof G50 starch which results in survival of some double helices and micron-scale structures (detected by DSC, SEC) after cooking leads to a higher yield of ERS fraction compared with cooked NMS and WMS. Among three maize starch extrudates with different initial amylose contents, only high-amylose G50 starch shows relatively lower digestion rate and extent, compared with almost fully digested WMS and NMS extrudates (Figure 2 A).In particular, the large difference in digestion rates of G50 extrudates compared with cooking in excess water (Table 1), for materials with very similar and low indices of molecular and crystalline order (Table 2), provides strong evidence that non-ordered conformations are involved in the slow rate of digestion of G50 extrudates. The simplest explanation for this difference is that the extrusion process caused an increase in local density of non-ordered conformations which was not reversed on hydration.

From the electron micrographs of G50 extrudates before and after digestion presented in Figure 3 and previous reports (Shrestha, Blazek, Flanagan, Dhital, Larroque, Morell, et al., 2015; Shrestha, Ng, Lopez-Rubio, Blazek, Gilbert, & Gidley, 2010),it was found that all the granules weregrossly disrupted and deformed within the extruder by mechanical force and heat/moisture induced swelling. Therefore,there was more homogeneity in the digestion pattern in contrast to native starch.Recently, Shrestha, et al. (2015) suggested that the digestion-limiting features in extruded starches are molecular and/or mesoscopic factors rather than the granular level, although the physical architecture of extrudates also can act as a barrier to prevent enzyme access to some extent.Size fraction did not markedlyinfluence the digestion kinetic profiles (Figure 2 B, C), indicating thatenzymic hydrolysis of fine and medium size fractions for NMS and G50 extrudates washydrolysis-limited rather than access/binding-limited. However, a small amount ofcoarseaggregates frombothextrudates(yield <ca.

509 15%) shows much lower digestibility, probably due to the effect of diffusion barriers to enzyme
510 access.
511
512 Wealso investigated the changes in starchmolecularcomposition and organization that occurred after
513 extrusion and digestion, including molecular size distributions, double/single helical and crystallinity
514 levels, and thermal properties.It is highly likely that the ordered features play some role in restricting
515 enzymic hydrolysis, as indicated by a small increase in double helical and crystallinity levels for
516 enzyme-resistant fractions of G50 extrudates after 2 h digestion (Table 2). Lopez-Rubio, Flanagan,
517 Shrestha, Gidley, and Gilbert (2008)suggestedthat the characteristic dimension of the resistant
518 crystals formed was ~5 nm with a maximum DP of ~13 and ~17 glucose units for double and single
519 helices respectively. These ordered structures were later suggested to be associated with some highly
520 branched amorphous fringed ends coating on the surface of double helices, providing a physical
521 barrier to enzyme access/binding whichslows the digestion rate (Shrestha, et al., 2015).However,
522 almost amorphous starch matrices were achieved by extruding G50 starch under the conditions used
523 here, with fractions being ca. 90% amorphous (judged by NMR and XRD).These non-crystalline
524 chains from high-amylose starches can pack in an enzyme-resistant form following extrusion
525 processingand deliver slow digestion rate, consistent with previous findings(Chanvrier,
526 Uthayakumaran, Appelqvist, Gidley, Gilbert, & Lopez-Rubio, 2007; Htoon, et al., 2009).This
527 suggests thatthe local molecular density (packing) of starch chains can control the digestion
528 rate/extent within low-order starch materials,crystallinity alone may not be sufficient to explain
529 enzyme resistance(Htoon, et al., 2009), and tightly packed non-crystalline regions can also be
530 enzyme resistant, provided they are constrained from swelling extensively in water.Comparison of
531 G50 starches in cooked and extrudate forms, showed some differences in both fully branched and
532 debranched SEC weight distributions ofresidues recovered after 2 h digestion. The debranched SEC
533 weight distributions of these two digestion residues cover a broad range of chain lengths (Figure 5C,

D). It is noteworthy that more long chain polymers (R_h> 10 nm, DP > 500) survived, in agreement with the fully branched size distributions (Figure 5 G, H).These SEC results are consistent with longer chain polymers (presumably from native or degraded amylose molecules) conferring relatively higher local molecular density in the original G50 extrudates.

The non-crystallineoramorphous state is based on the absence of detectable molecular order, butentanglements of amorphous glucan chains can give rise to tightly packed non-ordered matrices increasing localized molecular density. Another example of such locally-dense non-ordered starch structures is in the surface envelope of granule 'ghosts': the residual undissolved fraction of starch granules cooked in excess water with limited shear (Zhang, Dhital, Flanagan, & Gidley, 2014).However, thetechnical measurement of local molecular density to quantify sub-micron variability of starch matrices is challenging, and would be the key to studyingthe structural origins of enzyme resistance from amorphous conformation.Some attempts have been made to measure the free-volume radius distribution of polymeric materialsranging from nanometer to sub-micrometer length scale by positron annihilation lifetime spectroscopy, which is a potential technique to quantify the local molecular density(Liao, Chen, Awad, Yuan, Hung, Lee, et al., 2011).Comparingmolecular order (judged by NMR, XRD and DSC, Table 2) and relative enzyme digestion rates (Table 1)in cooked vs extruded starches,it was found that molecularorder/crystallinity contentsweresimilarly low (7 vs 9or 12% respectively by NMR) but enzyme resistance was much greater for extruded forms.We suggest that this is strong evidence that tightly packed amorphous material at the (sub)micrometer length scalehas a role to play in restricting enzyme action.

5. Conclusions

Three maize starches with different amylose contents were processed though extrusion with water

asthe sole plasticizer to achieve low-order starch matrices, with only extruded high-amylose starch exhibitinglower subsequentdigestion rate/extent. On the basis of NMR and XRD data,the double helix/crystallinity contents and melting temperatures of high-amylose starches in cooked and extruded forms were similar (ca. 80% amorphous fraction), but enzyme resistance was much greater for extruded forms. We suggest that the local density of packing of starch chains can control its digestibility rather than just crystallinity, which represents only one mechanism of achieving high local density of packing. If these molecularly dense structures are on about a (sub)micron length scale or longer, they could restrictenzyme actionin the small intestine with potential health benefits.

Appendix A. Supplementary data

Supplementary data associated with this article can be found in the online version.

Acknowledgements

The authors thank the facilities, and the scientific and technical assistance of Dr. Kim Sewell, of the Australian Microscopy & Microanalysis Research Facility at the Centre for Microscopy and Microanalysis, The University of Queensland.Dr. John Milne is acknowledgedfor his assistance with extrusion work. This study was partly supported by Australian Research Council Discovery Grant DP130102461.

References

Bird, A. R., Lopez-Rubio, A., Shrestha, A. K., & Gidley, M. J. (2009). Resistant starch in vitro and in vivo: Factors determining yield, structure, and physiological relevance. In S. Kasapis, Norton, I. T., & Ubbink, J. B. (Ed.), *Modern Biopolymer Sciences,* (pp. 449–510). London: Academic Press.

582 Butterworth, P. J., Warren, F. J., Grassby, T., Patel, H., & Ellis, P. R. (2012). Analysis of starch
583 amylolysis using plots for first-order kinetics. *Carbohydrate Polymers, 87*(3), 2189-2197.
584 Cairns, P., Sun, L., Morris, V. J., & Ring, S. G. (1995). Physicochemical studies using amylose as an
585 in vitro model for resistant starch. *Journal of Cereal Science, 21*(1), 37-47.
586 Cave, R. A., Seabrook, S. A., Gidley, M. J., & Gilbert, R. G. (2009). Characterization of starch by
587 size-exclusion chromatography: The limitations imposed by shear scission. *Biomacromolecules,*
588 *10*(8), 2245-2253.
589 Chanvrier, H., Uthayakumaran, S., Appelqvist, I. A. M., Gidley, M. J., Gilbert, E. P., & Lopez-
590 Rubio, A. (2007). Influence of storage conditions on the structure, thermal behavior, and formation
591 of enzyme-resistant starch in extruded starches. *Journal of Agricultural and Food Chemistry, 55*(24),
592 9883-9890.
593 Cheetham, N. W. H., & Tao, L. P. (1998). Variation in crystalline type with amylose content in
594 maize starch granules: an X-ray powder diffraction study. *Carbohydrate Polymers, 36*(4), 277-284.
595 Clay, P. A., & Gilbert, R. G. (1995). Molecular-weight distributions in free-radical polymerizations
596 .1. Model development and implications for data interpretation. *Macromolecules, 28*(2), 552-569.
597 Dhital, S., Warren, F. J., Butterworth, P. J., Ellis, P. R., & Gidley, M. J. (2015). Mechanisms of
598 starch digestion by alpha-amylase: Structural basis for kinetic properties. *Critical Reviews in Food*
599 *Science and Nutrition*, doi: 10.1080/10408398.10402014.10922043.
600 Englyst, H. N., & Cummings, J. H. (1985). Digestion of the polysaccharides of some cereal foods in
601 the human small-intestine. *American Journal of Clinical Nutrition, 42*(5), 778-787.
602 Faraj, A., Vasanthan, T., & Hoover, R. (2004). The effect of extrusion cooking on resistant starch
603 formation in waxy and regular barley flours. *Food Research International, 37*(5), 517-525.
604 Gidley, M. J., Hanashiro, I., Hani, N. M., Hill, S. E., Huber, A., Jane, J. L., Liu, Q., Morris, G. A.,
605 Rolland-Sabate, A., Striegel, A. M., & Gilbert, R. G. (2010). Reliable measurements of the size

606 distributions of starch molecules in solution: Current dilemmas and recommendations. *Carbohydrate*
607 *Polymers, 79*(2), 255-261.
608 Gilbert, R. G., Gidley, M. J., Hill, S., Kilz, P., Rolland-Sabate, A., Stevenson, D. G., & Cave, R. A.
609 (2010). Characterizing the size and molecular weight distribution of starch: Why it is important and
610 why it is hard. *Cereal Foods World, 55*(3), 139-143.
611 Godet, M. C., Buleon, A., Tran, V., & Colonna, P. (1993). Structural features of fatty acid-amylose
612 complexes. *Carbohydrate Polymers, 21*(2-3), 91-95.
613 Hoover, R., & Ratnayake, W. S. (2001). Determination of total amylose content of starch. In R. E.
614 Wrolstad, T. E. Acree, E. A. Decker, M. H. Penner, D. S. Reid, S. J. Schwartz, C. F. Shoemaker, D.
615 Smith, & P. Sporns (Eds.), Current protocols in food analytical chemistry - Water, protein, enzymes,
616 lipids and carbohydrates. Hoboken: Wiley-Interscience. pp. 689-691.
617 Htoon, A., Shrestha, A. K., Flanagan, B. M., Lopez-Rubio, A., Bird, A. R., Gilbert, E. P., & Gidley,
618 M. J. (2009). Effects of processing high amylose maize starches under controlled conditions on
619 structural organisation and amylase digestibility. *Carbohydrate Polymers, 75*(2), 236-245.
620 Jiang, H., Horner, H. T., Pepper, T. M., Blanco, M., Campbell, M., & Jane, J.-l. (2010). Formation of
621 elongated starch granules in high-amylose maize. *Carbohydrate Polymers, 80*(2), 533-538.
622 Lai, L. S., & Kokini, J. L. (1991). Physicochemical changes and rheological properties of starch
623 during extrusion. *Biotechnology Progress, 7*(3), 251-266.
624 Li, M., Hasjim, J., Xie, F. W., Halley, P. J., & Gilbert, R. G. (2014). Shear degradation of molecular,
625 crystalline, and granular structures of starch during extrusion. *Starch-Starke, 66*(7-8), 595-605.
626 Liao, K. S., Chen, H. M., Awad, S., Yuan, J. P., Hung, W. S., Lee, K. R., Lai, J. Y., Hu, C. C., &
627 Jean, Y. C. (2011). Determination of free-volume properties in polymers without orthopositronium
628 components in positron annihilation lifetime spectroscopy. *Macromolecules, 44*(17), 6818-6826.
629 Liu, W. C., Halley, P. J., & Gilbert, R. G. (2010). Mechanism of degradation of starch, a highly
630 branched polymer, during extrusion. *Macromolecules, 43*(6), 2855-2864.

631 Lopez-Rubio, A., Flanagan, B. M., Gilbert, E. P., & Gidley, M. J. (2008). A novel approach for
632 calculating starch crystallinity and its correlation with double helix content: A combined XRD and
633 NMR study. *Biopolymers, 89*(9), 761-768.
634 Lopez-Rubio, A., Flanagan, B. M., Shrestha, A. K., Gidley, M. J., & Gilbert, E. P. (2008). Molecular
635 rearrangement of starch during in vitro digestion: Toward a better understanding of enzyme resistant
636 starch formation in processed starches. *Biomacromolecules, 9*(7), 1951-1958.
637 Lopez-Rubio, A., Htoon, A., & Gilbert, E. P. (2007). Influence of extrusion and digestion on the
638 nanostructure of high-amylose maize starch. *Biomacromolecules, 8*(5), 1564-1572.
639 Moretti, R., & Thorson, J. S. (2008). A comparison of sugar indicators enables a universal high-
640 throughput sugar-1-phosphate nucleotidyltransferase assay. *Analytical Biochemistry, 377*(2), 251-
641 258.
642 Nishida, C., Uauy, R., Kumanyika, S., & Shetty, P. (2004). The joint WHO/FAO expert consultation
643 on diet, nutrition and the prevention of chronic diseases: process, product and policy implications.
644 *Public health nutrition, 7*(1a), 245-250.
645 Ranawana, V., Clegg, M. E., Shafat, A., & Henry, C. J. (2011). Postmastication digestion factors
646 influence glycemic variability in humans. *Nutrition Research, 31*(6), 452-459.
647 Shrestha, A. K., Blazek, J., Flanagan, B. M., Dhital, S., Larroque, O., Morell, M. K., Gilbert, E. P., &
648 Gidley, M. J. (2015). Molecular, mesoscrpic and microscopic tructure evolution during amylase
649 digestion of extruded maize and high-amylose maize starches. *Carbohydrate Polymers, 118*, 224-
650 234.
651 Shrestha, A. K., Ng, C. S., Lopez-Rubio, A., Blazek, J., Gilbert, E. P., & Gidley, M. J. (2010).
652 Enzyme resistance and structural organization in extruded high amylose maize starch. *Carbohydrate*
653 *Polymers, 80*(3), 699-710.

654 Tan, I., Flanagan, B. M., Halley, P. J., Whittaker, A. K., & Gidley, M. J. (2007). A method for
655 estimating the nature and relative proportions of amorphous, single, and double-helical components
656 in starch granules by C-13 CP/MAS NMR. *Biomacromolecules, 8*(3), 885-891.
657 Wang, K., Hasjim, J., Wu, A. C., Henry, R. J., & Gilbert, R. G. (2014). Variation in amylose fine
658 structure of starches from different botanical sources. *Journal of Agricultural and Food Chemistry,*
659 *62*(19), 4443-4453.
660 Warren, F. J., Zhang, B., Waltzer, G., Gidley, M. J., & Dhital, S. (2015). The interplay of alpha-
661 amylase and amyloglucosidase activities on thedigestion of starch in in vitro enzymic systems.
662 *Carbohydrate Polymers, 117*, 192-200.
663 Xie, F. W., Flanagan, B. M., Li, M., Sangwan, P., Truss, R. W., Halley, P. J., Strounina, E. V.,
664 Whittaker, A. K., Gidley, M. J., Dean, K. M., Shamshina, J. L., Rogers, R. D., & McNally, T.
665 (2014). Characteristics of starch-based films plasticised by glycerol and by the ionic liquid 1-ethyl-3-
666 methylimidazolium acetate: A comparative study. *Carbohydrate Polymers, 111*, 841-848.
667 Zhang, B., Dhital, S., Flanagan, B. M., & Gidley, M. J. (2014). Mechanism for starch granule ghost
668 formation deduced from structural and enzyme digestion properties. *Journal of Agricultural and*
669 *Food Chemistry, 62*(3), 760-771.
670 Zhang, B., Dhital, S., & Gidley, M. J. (2013). Synergistic and antagonistic effects of α-amylase and
671 amyloglucosidase on starch digestion. *Biomacromolecules, 12*(6), 1945-1954.
672 Zhang, B., Dhital, S., & Gidley, M. J. (2015). Densely packed matrices as rate determining features
673 in starch hydrolysis. *Trends in Food Science & Technology, 43*, 18-31.
674 Zhang, B., Huang, Q., Luo, F. X., & Fu, X. (2012). Structural characterizations and digestibility of
675 debranched high-amylose maize starch complexed with lauric acid. *Food Hydrocolloids, 28*(1), 174-
676 181.
677 Zhang, G. Y., Ao, Z., & Hamaker, B. R. (2006). Slow digestion property of native cereal starches.
678 *Biomacromolecules, 7*(11), 3252-3258.